ARTICLE

Streptozotocin-induced partial beta cell depletion in nude mice without hyperglycaemia induces pancreatic morphogenesis in transplanted embryonic stem cells

F. Takeshita · M. Kodama · H. Yamamoto · Y. Ikarashi ·
S. Ueda · T. Teratani · Y. Yamamoto · T. Tamatani ·
S. Kanegasaki · T. Ochiya · G. Quinn

Abstract

Aims/hypothesis It appears that the adult pancreas has limited regenerative ability following beta cell destruction by streptozotocin (STZ). However, it is not clear if this limitation is due to an inability to respond to, rather than an absence of, regenerative stimuli. In this study we aimed to uncouple the regenerative signal from the regenerative response by using an exogenous stem cell source to detect regenerative stimuli produced by the STZ-injured pancreas at physiological blood glucose levels.
Method Adult nude mice received 150 mg/kg STZ and 1×10^6 J1 mouse embryonic stem (ES) cells by i.p. injection. Permanent beta cell depletion of 50% was estimated from the ratio of beta:alpha cells in pancreata from STZ-treated mice compared with control animals after 24 days.
Results Transplanted ES cells homed to the STZ-injured pancreas and formed tumours. Immunocytochemical analysis of pancreas-associated ES tumours revealed foci con-

taining insulin/PDX-1 double-positive and glucagon-positive/PDX-1-negative cell clusters associated with PDX-1-positive columnar lumenal epithelium and extensive α-amylase-positive pancreatic acini comprising approximately 0.1% of ES tumour volume.
Conclusions/interpretation These data indicate that (1) the adult pancreas produces a milieu of regenerative stimuli following beta cell destruction, and (2) this is not dependent on hyperglycaemic conditions; (3) these regenerative stimuli appear to recapitulate the signalling pathways of embryonic development, since both exocrine and endocrine lineages are produced from PDX-1-positive precursor epithelium. This model will be useful for characterising the regenerative mechanisms in the adult pancreas.

Abbreviations
DAPI	4′,6-diamidino-2-phenylindole
E	embryonic day
ES	embryonic stem (cells)
ESM	Electronic supplementary material
IVIS	in vivo imaging system
PDX-1	pancreatic and duodenal homeobox protein-1
STZ	streptozotocin

F. Takeshita · M. Kodama · H. Yamamoto · S. Ueda · T. Teratani ·
Y. Yamamoto · T. Ochiya · G. Quinn (✉)
Section for Studies on Metastasis,
National Cancer Center Research Institute,
1-1 Tsukiji, 5-chome, Chuo-ku,
Tokyo 104-0045, Japan
e-mail: garyquinn99@hotmail.com

T. Tamatani · S. Kanegasaki · G. Quinn
Effector Cell Institute, Research Center for Advanced
Science and Technology (RCAST), University of Tokyo,
Tokyo, Japan

Y. Ikarashi
Pharmacology Division,
National Cancer Center Research Institute,
Tokyo, Japan

Introduction

Current mainstream treatments for type 1 (insulin-dependent) diabetes are frequently dogged by risks of hypoglycaemic episodes, increased body weight and numerous lifestyle restrictions [1]. On the other hand, type 2 (non-

insulin-dependent) diabetes is spreading at an epidemic pace in the developing world. Hence, there is a pressing need for superior treatments, which will benefit from deciphering the mechanisms of islet beta cell regeneration. The adult pancreas has the ability to regenerate following injury by a variety of means, although this regenerative capacity appears to be limited [2–5].

Streptozotocin (STZ) is a glucose-conjugated nitrosourea taken up via the pancreas-specific GLUT2 transporter. A single high dose of STZ can induce acute hyperglycaemia by rapid necrosis of pancreatic beta cells within 24 h [3], while multiple low doses of STZ can produce a gradual onset of hyperglycaemia by T cell-mediated autoimmune destruction of beta cells, a model sharing characteristics with type 1 diabetes [6]. Early studies in the hyperglycaemic rodent indicated that following a high dose of STZ, some but not significant numbers of beta cells were recovered [7]. A lower dose of STZ, producing less severe hyperglycaemia, resulted in permanent beta cell damage with negligible replacement of beta cells from the duct [8, 9]. However, it is not clear from these studies whether the lack of beta cell recovery in STZ-treated animals with normal blood glucose levels resulted from an absence of regenerating factors or from an inability of potential endogenous beta cell progenitors to respond to nascent regenerating stimuli.

We reported that following transplantation, undifferentiated mouse embryonic stem (ES) cells migrated to the liver and formed tumours in animals with hepatic injury [10]. These ES cell tumours contained differentiated hepatocytes induced by regenerating factors from the injured liver. The aim of the present study was to investigate the lack of beta cell recovery by introducing an exogenous multi-potent cell source to the nude mouse following a single STZ dose that induced partial beta cell destruction with neither the induction of hyperglycaemia nor the knock-on effect of T cell-mediated further beta cell damage.

We investigate whether moderate STZ-induced pancreatic injury can stimulate induction of pancreas morphogenesis in transplanted ES cells as well as self-regeneration. This approach could be important for unravelling the adult pancreas regeneration process and for identifying potential soluble factors for in vitro differentiation of insulin-producing beta cells for the treatment of diabetes.

Materials and methods

Animals and STZ treatment

Animal experiments in the present study were performed in compliance with the guidelines of the Institute for Laboratory Animal Research at the National Cancer Center

Research Institute (Tokyo, Japan). In addition, the Principles of Laboratory Animal Care (NIH publication no. 85-23, revised 1985; available from http://grants1.nih.gov/grants/olaw/references/phspol.htm, last accessed in July 2006) were followed. Female BALB/c nude mice (CLEA, Tokyo, Japan) aged 7 weeks were used as recipients for ES cell transplantation. Mice received a single 300-µl i.p. dose of STZ (Sigma Aldrich, St Louis, MO, USA) within 20 min of dissolution in freshly prepared 20 mmol/l cold citrate buffer (pH 4.5) at a dose ranging from 100 to 200 mg/kg body weight. Control mice received 300 µl citrate buffer alone. Duplicate glucose measurements were performed on whole venous blood collected from the tail vein of non-fasting animals at 48 h after STZ treatment and twice weekly thereafter, using the Freestyle Flash Blood Monitoring System (Nipro, Tokyo, Japan) according to the manufacturer's instructions. For investigation of the effect of STZ concentration on ES cell differentiation, 12 mice were used. Mice received ES cells 24 h after STZ injection by i.p. administration. All ES cells were injected on the same day and from the same cell preparation. The cell injection site was the lower abdomen, as far from the pancreas as possible. Physiological sample data at day 14 for these animals is shown in Table 1. For renal capsule transplantation experiments, 1×10^6 ES cells were transplanted 24 h following treatment of mice with 150 mg/kg STZ ($n=2$) or citrate buffer ($n=2$). Briefly, recipient mice were anaesthetised by exposure to 1–3% isoflurane, and a 1.5-cm cut through the skin and muscle of the left flank

Table 1 Physiological characteristics of animals transplanted i.p. with mouse embryonic stem cells

STZ treatment	Blood glucose (mmol/l)[a,b]	Weight (g)[a]	ES homing to pancreas?[a]
Citrate buffer #1	4.2	21.6	No
Citrate buffer #2	4.4	20.4	No
Citrate buffer #3	5.0	21.9	No
STZ 100 mg/kg #1	6.6	23.3	No
STZ 100 mg/kg #2	6.7	21.6	No
STZ 100 mg/kg #3	6.2	22.8	No
STZ 150 mg/kg #1	6.2	20.2	Yes
STZ 150 mg/kg #2	4.9	21.2	Yes
STZ 150 mg/kg #3	5.0	20.2	Yes
STZ 200 mg/kg #1	8.7	20.5	Yes
STZ 200 mg/kg #2	21.7	17.3	Yes
STZ 200 mg/kg #3	19.6	17.4	Yes

Relationship between STZ dose, blood glucose concentration (>11.1 mmol/l=hyperglycaemic) and effect on homing to the pancreas of transplanted mouse ES cells measured by in vivo imaging. Representative data is shown for mice at day 14. Blood glucose concentration remained similar to day 14 values for each animal until mice were killed on day 24. Average weight of mice at day 0=19±1 g.
[a] At day 14 post-treatment
[b] Average of two consecutive readings

dorsal to the spleen was made. The exposed wound was flushed with 1 ml PBS containing penicillin/streptomycin (Invitrogen, Carlsbad, CA, USA) and the kidney was pushed through the wound. A small cut was made laterally on the kidney membrane using a scalpel, and 10 μl PBS containing 1×10^6 ES cells was gently expelled towards the bottom of the kidney capsule using a 20-μl pipette tip. The kidney was replaced in the abdominal cavity, and the incision was closed with small wound clips. For i.v. transplantation, 1×10^6 ES cells in 100 μl PBS were injected via the tail vein 24 h after STZ treatment. For evaluation of induction of hormone-positive duct cells in the pancreas of STZ-treated mice, animals were treated with citrate buffer (group 1, n=3), 150 mg/kg STZ (group 2, n=6) or 200 mg/kg STZ (group 3, n=6), and killed 24, 48 and 72 h later (one in group 1, two in group 2, three in group 3 for each time point), and tissues were sectioned and stained for glucagon and insulin.

For estimation of permanent beta cell depletion in 150 mg/kg STZ- vs citrate buffer-injected mice, six animals were used. Mice were treated with 150 mg/kg STZ (n=3) or citrate buffer (n=3) and killed after 24 days, then pancreas sections were double-stained using immunofluorescence for glucagon and insulin as described below. All six mice had blood glucose concentrations <11.1 mmol/l throughout the 24-day period. Islets containing between 10 and 400 cells for each animal were photographed, and alpha and beta cells were counted using ImageJ software (version 1.31v) available from http://rsb.info.nih.gov/ij/download.html, last accessed in July 2006. For each islet, the ratio of beta:alpha cells was calculated and averaged for >30 islets per mouse (100 islets per group). For evaluation of the percentage of ES cell tumours occupied by pancreatic foci and PDX-1-positive foci ImageJ software was used to draw a closed perimeter around the foci and measure the sum of the areas occupied by these foci relative to the area of a closed perimeter drawn around the whole tissue section. This was repeated for several tissue sections from each mouse and averaged. For estimation of numbers of insulin-positive and PDX-1/insulin double-positive cells, individual cells were counted within the closed perimeter area of the ES cell tumour pancreatic foci only and their overall ES cell tumour proportion was then estimated.

Culture and in vivo transplantation of ES cells

The firefly luciferase-expressing ESJ1 cell line, a J1 cell clone of 129SV male origin, was established as described previously [11]. Twenty-four hours after STZ treatment, mice received 1×10^6 ES cells by single i.p. injection in 300 μl PBS prepared as described previously [11]. In vivo imaging analysis of transplanted ES cells was conducted in a cryogenically cooled IVIS system (Xenogen, Alameda,

CA, USA). Mice were administered D-luciferin (150 mg/kg; Promega, Madison, WI, USA) by i.p. injection and anaesthetised by exposure to 1–3% isoflurane. Photons from animal whole bodies were counted 10 min later using the IVIS imaging system according to the manufacturer's instructions, and data were analysed using LIVINGIMAGE 2.50 software (Xenogen). The amount of light generated was directly related to the amount of luciferase-producing cells. The development of pancreatic ES cell tumours was monitored twice weekly.

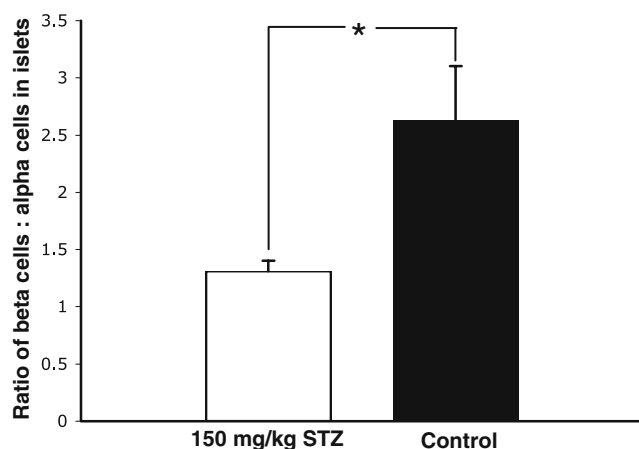Immunofluorescence and immunohistochemical analyses

Following killing of mice by cervical dislocation, pancreases and ES cell tumour tissues were preserved in 10% formalin solution, before being embedded in paraffin and sectioned. Sections were deparaffinised in xylene and rehydrated through a graded ethanol series. Antigen retrieval was performed by boiling sections for 5 min in 10 mmol/l citrate buffer followed by cooling for 30 min to room temperature. Blocking was carried out using Image-iT FX Signal Enhancer (Invitrogen) for 30 min at room temperature. Primary antibodies were applied overnight at 4°C. AlexaFluor secondary antibodies (1:1,000; Invitrogen) were applied for 30 min at room temperature. All antibodies were diluted in ChemMate Antibody Diluent (Dako, Kyoto, Japan). Immunofluorescence-stained sections were mounted with Vectashield mounting medium (Vector Laboratories, Burlingame, CA, USA) containing 4′, 6-diamidino-2-phenylindole (DAPI) to visualise nuclei. The following primary antibodies were used: anti-insulin (1:400, #MAB1417; R&D systems, Minneapolis, MN, USA), anti-glucagon (1:200, #sc-7779; Santa Cruz Biotechnology, Santa Cruz, CA, USA), anti-C-Peptide (1:400, #4023-01; Linco, St Charles, MO, USA), anti-HNF3β (1:100, #sc-9187; Santa Cruz) anti-PDX-1 (1:100, #07-696; Upstate, Charlottesville, VA, USA), anti-α-amylase (1:200, #A8273; Sigma) and anti-luciferase (1:100, #PM016; MBL, Woburn, MA, USA). Luciferase, HNF3β and α-amylase staining was performed using the Vectastain ABC kit (Vector Laboratories) according to the manufacturer's instructions, followed by haematoxylin or eosin counter-staining using standard methods.

Results

Beta cell neogenesis following STZ treatment

Doses of 150 mg/kg STZ or below consistently failed to induce overt hyperglycaemic blood glucose concentrations (>11.1 mmol/l) up to 4 weeks following treatment (Table 1; sample data is shown at day 14), while doses of 200 mg/kg

usually led to acute hyperglycaemia (blood glucose concentration >11.1 mmol/l) within 48 h, which was accompanied by sustained poor weight gain and polyuria thereafter. The lowest single STZ dose that can induce hyperglycaemia in mice is variable and dependent on genetic background for inbred strains. The BALB/c genetic background displays unusually high resistance to STZ-induced DNA damage, which is directly related to poly (ADP-ribose) polymerase (PARP) activation and NAD depletion [12]. This would explain why a STZ dose of 150 mg/kg, which is sufficient to induce rapid hyperglycaemia in some mouse strains, did not do so in this study. Nevertheless, since STZ degrades rapidly and mice treated with 150 mg/kg STZ did not develop elevated blood glucose levels in this study, an alternative method was necessary to establish that the STZ dose administered in this instance induced some degree of beta cell depletion. As STZ is a selective destroyer of beta cells, the alpha cell population should remain constant before and after treatment (unless there is an expansion of alpha cells during regeneration that has not previously been demonstrated). We therefore compared the average ratio of beta (insulin-positive): alpha (glucagon-positive) cells over a range of islet sizes from non-ES cell-transplanted control mice (n=3) and mice treated with 150 mg/kg STZ (n=3) 24 days after treatment. Using this approach we estimated that the average rate of permanent destruction of beta cells in euglycaemic mice treated with 150 mg/kg was 50% (Fig. 1). Between 24 and 48 h after 150 mg/kg STZ treatment, some ductal hormone-positive cells were detectable in the pancreas of treated mice, including occasional insulin/glucagon double-positive cells (data not shown). However, 24 days after treatment, hormone-positive duct

cells were not detectable. In contrast, in hyperglycaemic mice treated with 200 mg/kg STZ, clusters of insulin-positive cells within the pancreatic ducts were common after 24 days (data not shown), as previously observed in the regenerating adult pancreas under hyperglycaemic conditions [13].

Transplanted ES cells migrate to and proliferate in the STZ-injured pancreas

Pancreatic homing and proliferation of i.p. transplanted ES cells was clearly detectable by in vivo imaging in all animals that received doses of 150 mg/kg or 200 mg/kg STZ from day 14 after transplantation (Fig. 2). At lower STZ doses (100 mg/kg) and in citrate buffer-treated mice, homing to the pancreas was not detected in any animals up to day 24 when all mice were killed. Earlier attempts using i.v. transplantation of ES cells also gave rise to small peripancreatic tumours. However, these tumours developed more slowly than following i.p. transplantation (Electronic supplementary material [ESM] Fig. 1) and mice were prone to lethal pulmonary teratomas. All mice produced s.c. tumours at the site of injection, presumably due to some leaking of cells into the s.c. space during ES cell injection. In addition to s.c. tumours, small teratomas were occasionally observed at random sites (non-pancreas-associated) sites in the peritoneum of i.p. ES cell transplanted mice. Anatomical analysis of the pancreata of 150 mg/kg STZ-treated mice following killing at 24 days after ES cell injection revealed vascular networks interconnecting ES cell-derived tumour nodules with the vasculature of the host pancreas (Fig. 2), indicating that the movement of soluble factors between pancreas and ES cell tumour was facilitated during ES cell tumour growth and differentiation.

Transplanted ES cells differentiate into hormone-positive cell clusters in STZ-treated mice

ES cell-derived pancreatic tumours were analysed for expression of hormonal markers of pancreatic islet (alpha and beta) cells. Staining of serial ES cell tumour sections alternately for insulin and glucagon revealed foci with clusters of hormone-positive cells spatially associated with each other and arranged along the periphery of rosettes of large eosinophilic granular cells, which displayed histological similarity to pancreatic acini (Fig. 3c, inset). These acinar-like cells were hormone-negative. In addition, these ES cell tumour foci always contained lumenal columnar epithelium adjacent to the hormone-positive clusters. This epithelium showed weak hormone staining that was polarised towards the acinar-like and hormone-positive cell clusters and occasionally contained cells that stained strongly positive for glucagon or insulin (Fig. 3, arrowheads).


Fig. 1 Permanent beta cell depletion in the pancreatic islets of euglycaemic mice treated with STZ. Mice received 150 mg/kg STZ (*white bar*; n=3) or citrate buffer alone (*black bar*; n=3). The average ratio of beta (insulin-positive):alpha (glucagon-positive) cells in >100 islets per group at day 24 after STZ treatment revealed approximately 50% permanent beta cell depletion. Data are presented as means±SEM. *p<0.05, t test

Fig. 2 Pancreatic homing and expansion of ES cells in STZ-treated mice were monitored in vivo by bioluminescent imaging using the IVIS system. Day 14 (**a**–**d**) and day 24 (**e**–**h**) representative images of nude mice injected i.p. on day 0 with STZ at 200 mg/kg (**a**, **e**), 150 mg/kg (**b**, **f**), 100 mg/kg (**c**, **g**) or citrate buffer only (**d**, **h**), followed 24 h later by i.p. injection of 1×10^6 ES cells in 300 μl Dulbecco's PBS are shown; pancreas-associated ES cell tumours are indicated by arrowheads; all mice developed s.c. ES cell tumours at injection site (*arrows*). **i** At day 24, 150 mg/kg STZ dose, highly vascularised ES cell tumour nodules (T) were interconnected with the host pancreas vasculature (*). **j** confirmation of ES cell homing to pancreas by ex vivo imaging
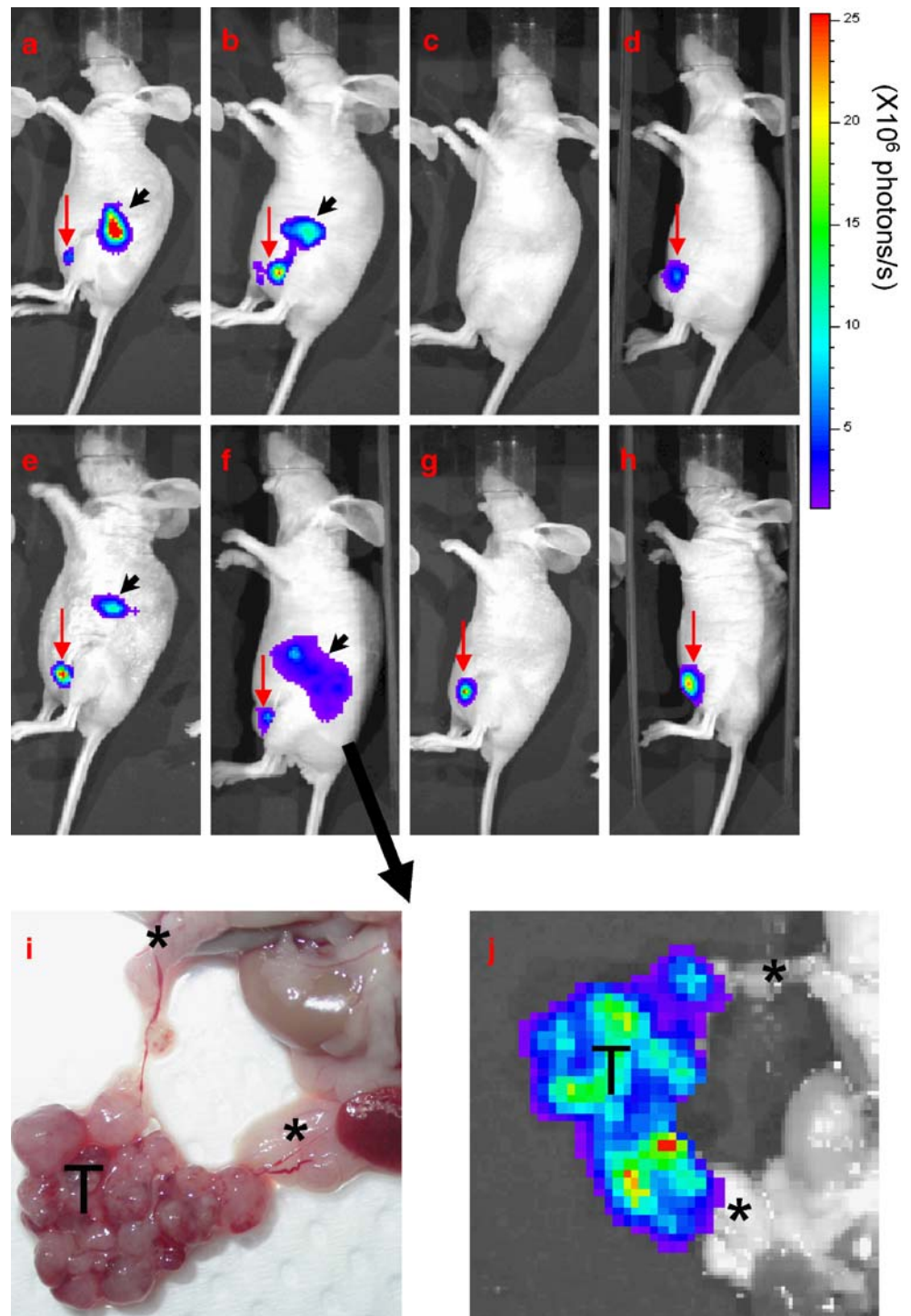
Insulin-positive cell clusters are associated with α-amylase-positive acinar cells in ES cell tumour foci, suggesting a common origin

Closer analysis of ES cell tumour foci revealed that insulin-positive cell clusters were located in close contact with α-amylase-positive acinar-like cells (Fig. 4). However, there was no overlap between α-amylase and insulin staining. The occurrence of endocrine and exocrine cells at common foci suggests that they originated from a common precursor cell type. Approximately 0.1% of the peri-pancreas teratomas comprised pancreatic foci that we define as cell clusters containing lumenal epithelial cells positive for α-amylase, insulin and PDX-1 in close association (Table 2). Furthermore, this tight arrangement of cells with distinguishable specialised functions is similar to that found
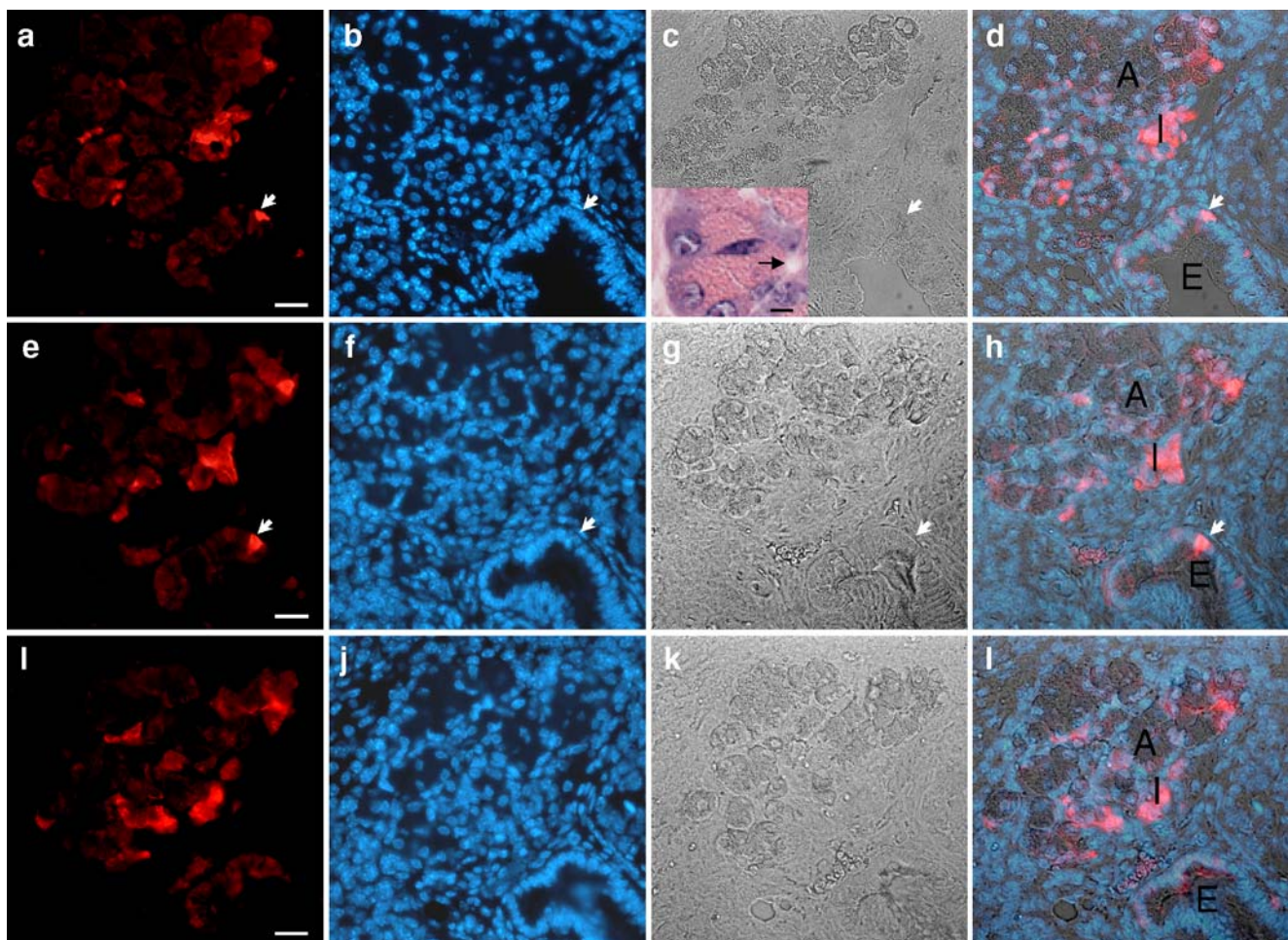
Fig. 3 Hormone-positive clusters are induced in ES cell tumours following 150 mg/kg STZ treatment. Serial sections of ES cell tumour foci were stained alternately for glucagon (*red*; **a–d**, **i–l**) and insulin (*red*; **e–h**). Hormone-positive cells were observed within the lumenal epithelium (E, *arrowheads*) and in adjacent islet-like clusters (I). In close proximity to the islet-like clusters were clusters of large granular cells with acinar-like cell morphology (A). **c** Inset (scale bar=5 μm) shows a haematoxylin and eosin photomicrograph of a segment of an ES cell tumour acinus. The pyramidal cell shape with nucleus at broad basal surface and eosinophilic zymogen granules in the apical cytoplasm towards the lumen (*arrow*) are clearly seen. **a**, **i** Glucagon; **e** insulin; **b**, **f**, **j** DAPI; **c**, **g**, **k** phase contrast; **d**, **h**, **l** hormone/DAPI/ phase contrast overlay. Scale bar=25 μm

in maturing islets and acini in the pancreas post embryonic day (E) 14.5, and occurred in proximity to simple columnar epithelium resembling endodermal gut epithelium.

ES cell tumour foci contain PDX-1-positive epithelium resembling pancreatic anlage

PDX-1 is the earliest marker of pancreatic stem cells that give rise to all three pancreatic lineages [14] and is essential for pancreatic morphogenesis. It is expressed almost uniformly in the dorsal and ventral pancreatic buds that evaginate from the ventral gut epithelium. Following lineage commitment, PDX-1 expression is lost in pancreas cells, and is re-expressed at high levels in mature beta cells as a key transactivator of beta cell-specific hormone expression. PDX-1 staining of lumenal epithelium in ES cell tumour foci revealed a high density of positive cells

(50%) (Fig. 5a). The PDX-1-positive epithelium was hormone- and α-amylase-negative, and displayed polarisation with distinct tracts of uniformly PDX-1-positive cells distinguishable from PDX-1-negative epithelial cells. Co-staining of foci for α-amylase revealed that this polarity was towards exocrine-like cells, which arose as a continuum of the PDX-1-positive epithelium, with a clear down-regulation of PDX-1 at the interface with cells undergoing induction of the gene for α-amylase. The α-amylase-positive cells were PDX-1-negative. We confirmed that PDX-1-positive foci originated from the endodermal lineage by co-staining for HNF3β (Fig. 5h). To determine whether ES cell tumours could undergo pancreatic morphogenesis in another well-vascularised location, we transplanted undifferentiated ES cells under the kidney capsule of 150 mg/kg STZ- (*n*=2) and citrate buffer-treated (*n*=2) mice (ESM Fig. 2). Approximately 2% of the kidney
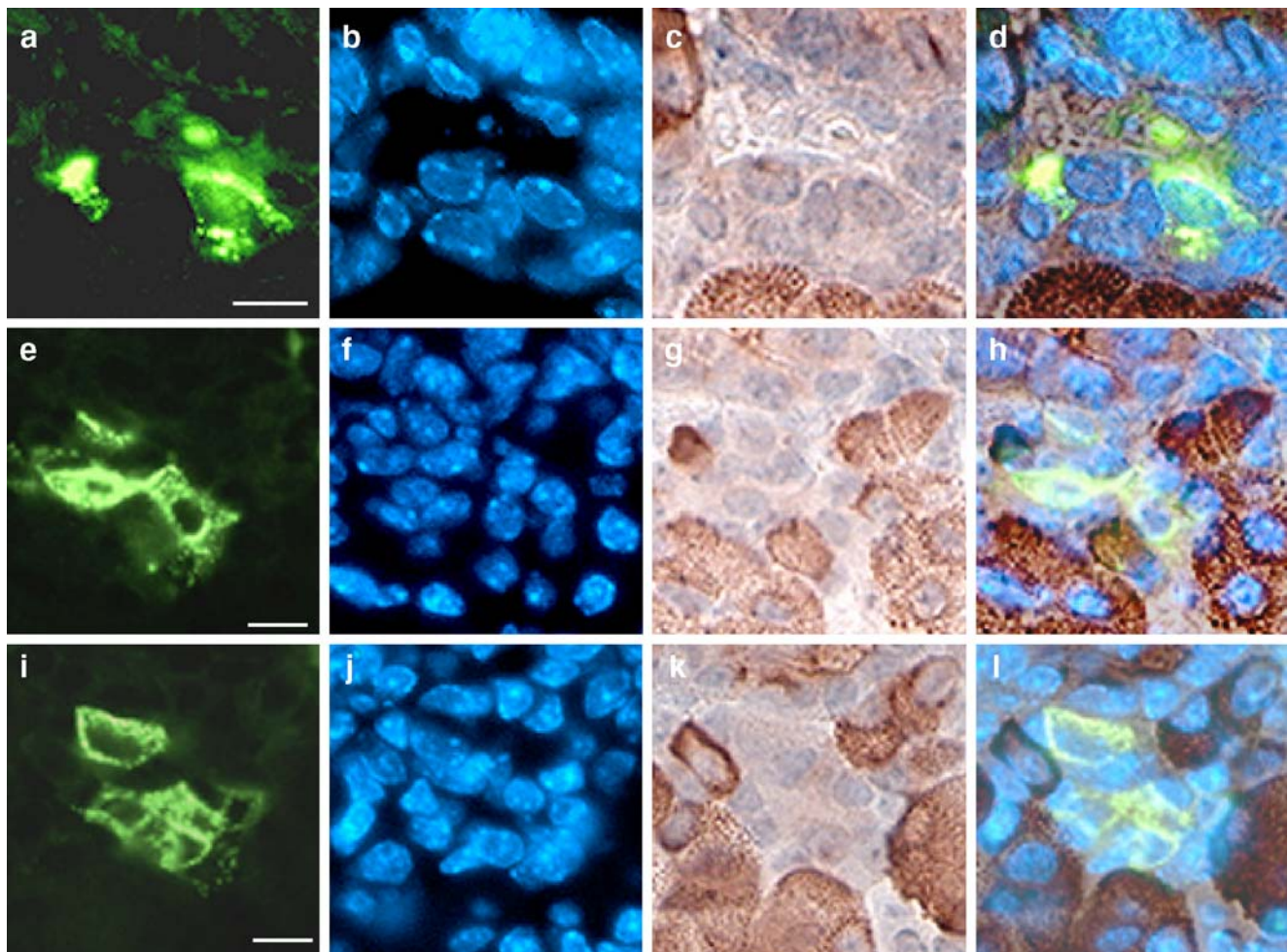
Fig. 4 Induction of beta cell-like clusters in ES cell tumour foci appears to follow a developmental pathway. Serial sections of tumour foci were stained for insulin (*green*) and α-amylase (*brown*). Clusters of insulin-positive cells appear in close association with α-amylase-positive acinar cells without overlap of marker expression. This arrangement is similar to that found in the later stages of pancreatic organogenesis (after E 14.5). **a**, **e**, **i** Insulin; **b**, **f**, **j** DAPI; **c**, **g**, **k** α-amylase; **d**, **h**, **l** insulin/DAPI/α-amylase overlay. Scale bars=5 μm

capsule ES cell tumour from the 150 mg/kg STZ-treated mice contained polarised PDX-1-positive luminal epithelium (ESM Fig. 3), compared with 0.1% of citrate buffer-treated mice (data not shown).

Table 2 Proportion of peri-pancreas ES tumours expressing pancreas-associated proteins

| Immunohistochemical marker	Percentage of peri-pancreas tumour
HNF3β	15±2.1
PDX-1	1.4±0.11
PDX-1/insulin/α-amylase[a]	0.1±0.022
PDX-1/insulin[b]	0.01±0.003

Data at day 24 following ES transplantation. Tumours from three mice were evaluated. Data is presented±SD. Peri-pancreas ES tumours expressing pancreas-associated proteins also expressed luciferase.
[a] Foci containing cells representing all three markers, either single- or double-positive. Average number of foci per tumour section=2
[b] Double-positive cells

ES cell tumour foci contain mature beta cells

To further characterise the pancreatic cells of our ES cell tumour foci we performed double-staining for C-peptide/PDX-1, insulin/PDX-1 and glucagon/PDX-1. During development, the majority of early insulin cells do not express PDX-1 when they first appear, but PDX-1 is later upregulated in the mature beta cells [15]. However, mature alpha cells, which are interspersed with beta cells in the mature islet, are PDX-1-negative. Figure 6a–h illustrates a strong PDX-1/insulin/C-peptide triple-positive mature beta cell located in an ES cell tumour focus but separate from the PDX-1-positive epithelium. Glucagon-positive putative alpha cells were PDX-1-negative but adjacent to PDX-1-positive cells (beta cells) in a similar arrangement to that found in pancreatic islets. To confirm that the ES cell tumour-derived beta cells were derived from the endodermal lineage, we demonstrated nuclear co-expression of the
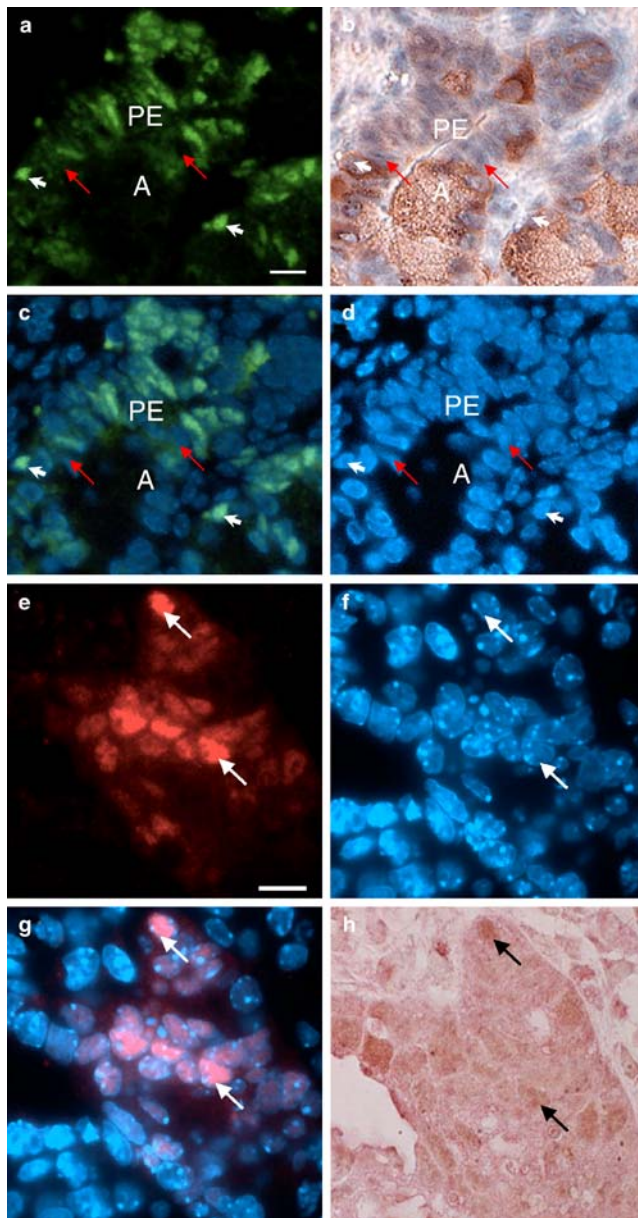
Fig. 5 a–d PDX-1 (*green*) is expressed in the nuclei of 50% of lumenal epithelial cells in ES cell tumour pancreatic foci. PDX-1-positive luminal epithelium is usually hormone-negative and is polarised towards α-amylase-positive (*brown*) acinar cells (A) which can be seen emerging as a continuum from the PDX-1-positive epithelium (PE) and cells at the interface show downregulation of PDX-1 expression (*arrows*). PDX-1-positive cells are also located outside the luminal epithelium (*arrowheads*). These cells are insulin-positive (not shown). **a** PDX-1; **b** α-amylase; **c** PDX-1/DAPI overlay; **d** DAPI. Scale bar=10 μm. **e–h** Co-localisation of PDX-1 and HNF3β proteins in pancreatic foci in ES cell tumours confirms their endodermal lineage. Sections of peri-pancreas tumours were stained for PDX-1 (*red*) and HNF3β (*brown*), both revealing nuclear local-isation. Examples of double-positive cells are indicated by arrows. **e** PDX-1; **f** DAPI; **g** PDX-1/DAPI overlay; **h** HNF3β. Scale bar=10 μm

HNF3β protein with PDX-1 and insulin (Fig. 6m–q). Finally, tissue sections were co-stained for luciferase along with glucagon and insulin to demonstrate that the hormone-positive cells observed in the ES cell tumours were indeed derived from the transplanted cells (Fig. 6r–v).

Discussion

The pancreas appears to lack the ability to sense its size, unlike the liver, and regeneration following pancreatectomy is incomplete [16]. Nevertheless, the observation that a range of stimuli can increase growth of acini [4, 17], ducts [5] and beta cells [2] suggests that there must be local signals capable of promoting growth in the postnatal animal. Following STZ treatment, irrespective of whether a high or low dose is used, beta cell replenishment is incomplete [9], which raises the possibility that regenerat-ing signals are present but the pancreas is incapable of an effective response.

We demonstrated here that when ES cells were intro-duced to mice with partial STZ-induced beta cell ablation, the cells migrated to the pancreas and proliferated, forming highly vascularised tumour nodules whose vasculature was connected to that of the host pancreas. These nodules contained cells with characteristics of endocrine (alpha and beta cells) and exocrine (α-amylase-positive) cells, indicat-ing that regenerative signals produced by the injured pancreas are capable of stimulating organ morphogenesis from precursor PDX-1-positive endodermal epithelium. This provides a clear demonstration, for the first time, that pancreatic beta cell ablation in the absence of hyper-glycaemia in the adult produces soluble signals that can recapitulate elements of embryonic pancreatic development.

In the mouse embryo, the pancreatic primordium is first visible at E 9.5 as an evagination of the foregut endoderm, consisting of a highly folded epithelial sheet with apical and basal surfaces continuous with those of the gut tube [18]. At this stage most of the cells express PDX-1, the master regulator of pancreas development [14], and glucagon-positive cells can be detected, although these first glucagon-positive cells are post-mitotic and do not contribute to the final alpha cell pool [18]. One day later, insulin-positive cells appear, and over the next 2–3 days, cells are frequently found to express both hormones together [19]. However, alpha and beta cells appear to be derived independently in the mouse pancreas [20]. At around E 14.5, exocrine cells become distinguishable from endocrine cells [18]. Endocrine cells are largely individual and associated with the ducts until the end of gestation (about E 18.5), when they are found as islets [18].
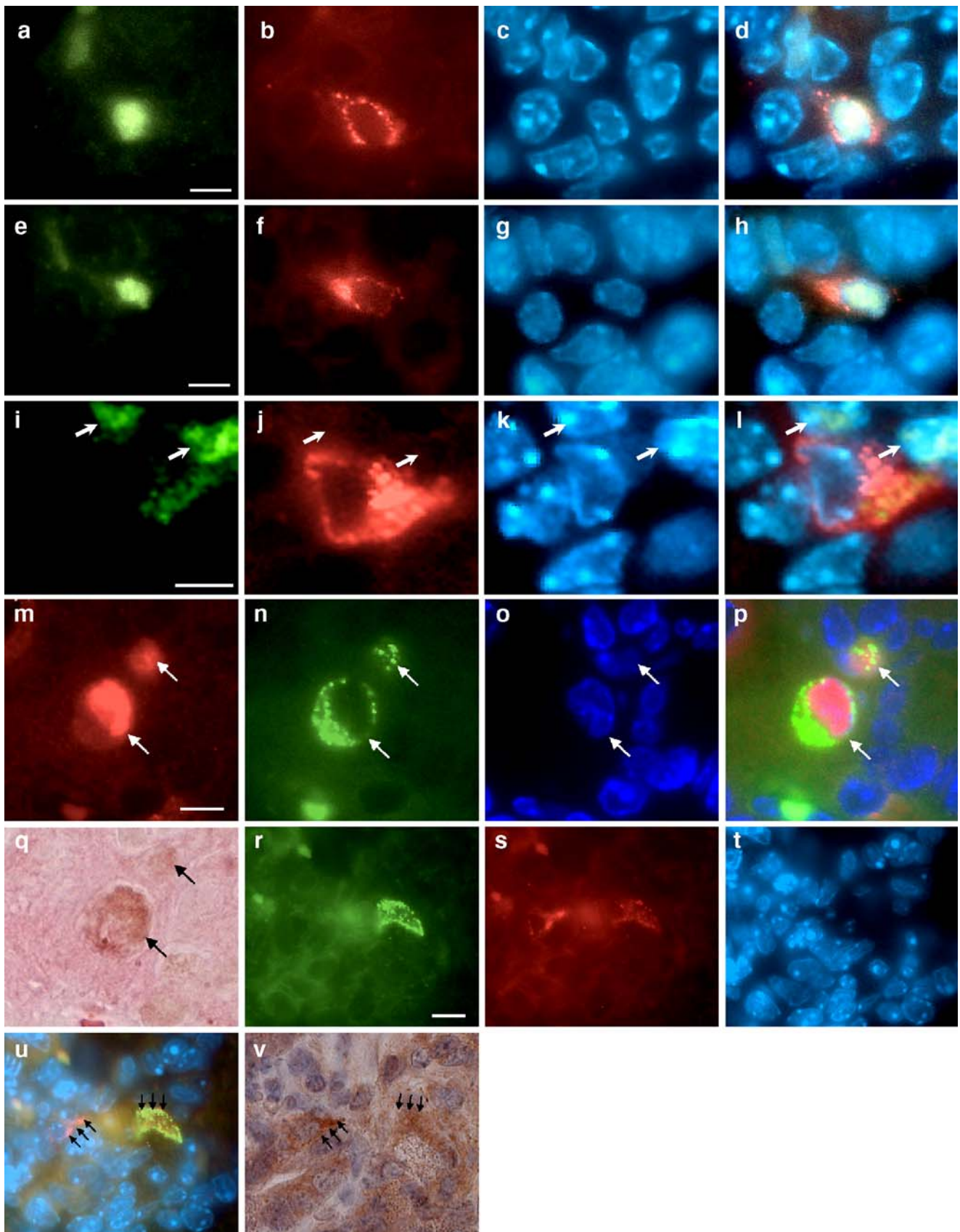
◀ **Fig. 6** Mature beta and alpha cells are found in ES cell tumour pancreatic foci. **a–d** and **e–h** represent serial sections. **a–d** and **i–l** represent the same tissue section. **a–c** PDX-1 (*green*), C-peptide (*red*), DAPI (*blue*); **d** PDX-1/C-peptide/DAPI overlay; **e–g** PDX-1 (*green*), insulin (*red*), DAPI (*blue*); **h** PDX-1/insulin/DAPI overlay; **i–k** PDX-1 (*green*), glucagon (*red*), DAPI (*blue*); **l** PDX-1/glucagon/ DAPI overlay showing a PDX-1-negative/glucagon-positive cell adjacent to PDX-1-positive/glucagon-negative beta cells (*arrows*) — both cell types have characteristics of mature pancreatic islet cells. Scale bars=5 μm. **m–q** Mature beta cells in ES cell tumours are induced from the endodermal lineage. HNF3β co-localises with PDX-1 in the nuclei of insulin-positive cells (*arrows*). **m** PDX-1; **n** insulin; **o** DAPI; **p** PDX-1/insulin/DAPI overlay; **q** HNF3β. Scale bar=5 μm. **r–v** Hormone-expressing cells in ES cell tumour pancreatic foci are induced from the transplanted cells. Luciferase staining is co-localised in hormone-expressing cells (*arrows*) from peri-pancreas ES cell tumour sections. **r** insulin (*green*); **s** glucagon (*red*); **t** DAPI (*blue*); **u** insulin/glucagon/DAPI overlay; **v** luciferase (*brown*). Scale bar=10 μm

The presence of PDX-1-positive lumenal epithelium, hormone-positive cell clusters and pancreatic acini in ES cell tumours indicates that the insulin-positive cells most likely arose from pancreas morphogenesis and not merely by cytodifferentiation. Additional support for this conclusion comes from both tissue reconstitution and genetic experiments [21–23] that have definitively demonstrated that pancreatic mesenchyme is required for exocrine, but not endocrine, differentiation. Subcutaneous ES cell tumours that formed at the ES cell injection site in both STZ-treated and non-treated mice revealed no evidence of pancreatic differentiation (data not shown), indicating that factors produced by the regenerating pancreas were required for the ES cell differentiation and suggesting that these factors may be more effective at close range.

In the pancreas itself, we observed evidence of inefficient beta cell neogenesis in 150 mg/kg STZ-treated animals, indicated by islets with altered beta:alpha cell ratios, as compared with control mice 24 days after treatment. Approximately half of islet beta cells were permanently lost following this treatment regimen. Although we have not measured the rate of insulin production in these injured islets, we found that normal glucose levels were maintained throughout a 24-day period. However, increasing the STZ dose to 200 mg/kg almost invariably induced rapid hyperglycaemia, suggesting that 150 mg/kg animals were close to exhibiting pathological blood glucose levels. In the present study our aim was to separate the secondary effects of high blood glucose, a known inducer of beta cell neogenesis, on its own in the absence of beta cell damage [24] from the primary effects of beta cell loss. Fernandes et al. [25] found that while a key subpopulation of intra-islet somatostatin/PDX-1 double-positive transitionary cells were expanded in mice following high-dose STZ treatment, low doses of STZ did not induce beta cell neogenesis, suggesting that the neogenic response observed

at high STZ doses was dependent on or related to elevated blood glucose levels. The rate of pancreatic foci and PDX-1/insulin double-positive cells was similar in peri-pancreas ES cell tumours from 200 mg/kg-treated mice (data not shown). However, since these mice were mildly hyperglycaemic (<22.2 mmol/l) we cannot yet remark on the effect of higher blood glucose concentrations (>22.2 mmol/l), nor the possibility of glucose-induced regenerative stimuli obscuring a reduction in beta cell loss-induced regenerative stimuli caused by the higher STZ doses required for induction of severe hyperglycaemia. That euglycaemic STZ-treated mice induced neogenesis of multiple lineages—islet and acinar—in exogenous multipotent cells strongly suggests that STZ-mediated beta cell damage, in the absence of hyperglycaemia, produces pancreas regeneration signals, although they apparently have limited effect in the adult pancreas itself since beta cell loss by the same STZ dose is never fully replenished. Our data raises the possibility that this lack of self-regeneration may be due to a limitation of the organ to respond to signals rather than an absence of regenerating stimuli per se. While it is unlikely that pancreatic morphogenesis depends on cell fusion between ES and host stem cells in this model, it cannot yet be ruled out that cell fusion events may occur that involve host cells such as macrophages, which are known to be relatively abundant in nude mice.

In conclusion, by uncoupling the regenerative signal produced by the damaged pancreas from the regenerative response, the model described here recapitulates elements of embryonic pancreas development in the injured adult pancreas. Future studies will focus on identification of factors produced by the injured pancreas. In addition, it will be important to characterise the response of putative adult beta stem cell types, such as bone marrow-derived mesenchymal stem cells [26] and intra-pancreatic stem cells [27, 28], to stimuli produced by the STZ-injured pancreas. This may be a valuable system for understanding the mechanisms of beta cell neogenesis in the adult and for identification of regenerative factors for use in tissue engineering in vitro.

Duality of interest The authors state that they have no duality of interest.

References

1. The Diabetes Control and Complications Trial Research Group (1997) Hypoglycemia in the Diabetes Control and Complications Trial. Diabetes 46:271–286

2. Gu D, Sarvetnick N (1997) Epithelial cell proliferation and islet neogenesis in IFN-γ transgenic mice. Development 118:33–46

3. Chang AY, Diani AR (1985) Chemically and hormonally induced diabetes mellitus. In: Volk BW, Arquilla ER (eds) The diabetic pancreas, 2nd edn. Plenum, New York, pp 415–438

4. Elsasser HP, Biederbick A, Hern HF (1994) Growth of rat pancreatic acinar cells quantitated with a monoclonal antibody against the proliferating cell nuclear antigen. Cell Tissue Res 276:603–609

5. Rosenberg L, Brown RA, Duguid WP (1983) A new approach to the induction of duct epithelial hyperplasia and nesidioblastosis by cellophane wrapping of the hamster pancreas. J Surg Res 35:63–72

6. Like AA, Rosini AA (1976) Streptozotocin-induced pancreatic insulitis: new model of diabetes mellitus. Science 193:415–417

7. Brosky G, Logothetopoulos J (1969) Streptozotocin diabetes in the mouse and the guinea pig. Diabetes 18:606–611

8. Steiner H, Oelz O, Zahnd G, Froesch ER (1970) Studies on islet cell regeneration, hyperplasia and intrainsular cellular interactions in long lasting streptozotocin diabetes in the rat. Diabetologia 6:558–564

9. Bonner-Weir S, Trent DF, Honey RN, Weir GC (1981) Responses of neonatal rat islets to streptozotocin. Diabetes 30:64–69

10. Yamamoto H, Quinn G, Asari A et al (2003) Differentiation of embryonic stem cells into hepatocytes: biological functions and therapeutic application. Hepatology 37:983–993

11. Teratani T, Yamomoto H, Aoyagi K et al (2005) Direct hepatic fate specification from mouse embryonic stem cells. Hepatology 41:836–846

12. Cardinal JW, Allan DJ, Cameron DP (1999) Poly(ADP-ribose) polymerase activation determines strain sensitivity to streptozotocin-induced beta cell death in inbred mice. J Mol Endocrinol 22:65–70

13. Bonner-Weir S (2000) Islet growth and development in the adult. J Mol Endocrinol 24:297–302

14. Jonsson J, Carlsson L, Edlund T, Edlund H (1994) Insulin-promoter-factor 1 is required for pancreas development in mice. Nature 371:606–609

15. Ohlsson H, Karlsson K, Edlund T (1993) IPF1, a homeodomain-containing transactivator of the insulin gene. EMBO J 12:4251–4259

16. Lehv M, Fitzgerald PJ (1968) Pancreatic acinar cell regeneration. IV. Regeneration after surgical resection. Am J Pathol 53:513–535

17. Jensen JN, Cameron E, Garay MVR, Starkey TW, Gianani R, Jensen J (2005) Recapitulation of elements of embryonic development in adult mouse pancreatic regeneration. Gastroenterology 128:728–741

18. Slack JMW (1995) Developmental biology of the pancreas. Development 121:1569–1580

19. Madsen OD, Jensen J, Blume N et al (1996) Pancreatic development and maturation of the islet β cell. Eur J Biochem 242:435–445

20. Jensen J, Heller R, Funder-Nielsen T et al (2000) Independent development of pancreatic α- and β-cells from neurogenin3-expressing precursors. Diabetes 49:163–176

21. Ahlgren U, Pfaff SL, Jessell TM, Edlund T, Edlund H (1997) Independent requirement for ISL1 in formation of pancreatic mesenchyme and islet cells. Nature 385:257–260

22. Wessells N, Cohen J (1966) Early pancreatic organogenesis: morphogenesis, tissue interactions, and mass effects. Dev Biol 15:237–270

23. Rose M, Crisera C, Colen K, Connelly PR, Longaker M, Gittes G (1999) Epithelio-mesenchymal interactions in the developing pancreas: morphogenesis of the adult architecture. J Pediatr Surg 34:774–779

24. Lipsett M, Finegood DT (2002) β-Cell neogenesis during prolonged hyperglycemia in rats. Diabetes 51:1834–1841

25. Fernandes A, King LC, Guz Y, Stein R, Wright CVE, Teitelman G (1997) Differentiation of new insulin-producing cells is induced by injury in adult pancreatic cells. Endocrinology 138:1750–1762

26. Sordi V, Malosio ML, Marchesi F et al (2005) Bone marrow mesenchymal stem cells express a restricted set of functionally active chemokine receptors capable of promoting migration to pancreatic islets. Blood 106:417–427

27. Seaberg RM, Smukler SR, Kieffer TJ et al (2004) Clonal identification of multipotent precursors from adult mouse pancreas that generate neural and pancreatic lineages. Nat Biotechnol 22:1115–1124

28. Hao E, Tyrberg B, Itkin-Ansari P et al (2006) Beta-cell differentiation from nonendocrine epithelial cells of the adult human pancreas. Nat Med 12:310–316